

DEVELOPMENT OF A MULTI- LOOP FLOW AND HEAT TRANSFER FACILITY FOR ADVANCED NUCLEAR REACTOR THERMAL HYDRAULIC AND HYBRID ENERGY SYSTEM STUDIES

IMECE2014

James E. O'Brien, Piyush Sabharwall,
SuJong Yoon

September 2014

The INL is a
U.S. Department of Energy
National Laboratory
operated by
Battelle Energy Alliance



This is a preprint of a paper intended for publication in a journal or proceedings. Since changes may be made before publication, this preprint should not be cited or reproduced without permission of the author. This document was prepared as an account of work sponsored by an agency of the United States Government. Neither the United States Government nor any agency thereof, or any of their employees, makes any warranty, expressed or implied, or assumes any legal liability or responsibility for any third party's use, or the results of such use, of any information, apparatus, product or process disclosed in this report, or represents that its use by such third party would not infringe privately owned rights. The views expressed in this paper are not necessarily those of the United States Government or the sponsoring agency.

IMECE2014-39057

**DEVELOPMENT OF A MULTI-LOOP FLOW AND HEAT TRANSFER FACILITY
FOR ADVANCED NUCLEAR REACTOR THERMAL HYDRAULIC AND HYBRID
ENERGY SYSTEM STUDIES**

James E. O'Brien, Piyush Sabharwall, SuJong Yoon
Idaho National Laboratory
Idaho Falls, Idaho, USA

ABSTRACT

A new high-temperature multi-fluid, multi-loop test facility for advanced nuclear applications is under development at the Idaho National Laboratory. The facility will include three flow loops: high-temperature helium, molten salt, and steam/water. Molten salts have been identified as excellent candidate heat transport fluids for primary or secondary coolant loops, supporting advanced high temperature and small modular reactors (SMRs). Details of some of the design aspects and challenges of this facility, which is currently in the conceptual design phase, are discussed. A preliminary design configuration will be presented, with the required characteristics of the various components. The loop will utilize advanced high-temperature compact printed-circuit heat exchangers (PCHEs) operating at prototypic intermediate heat exchanger (IHX) conditions. The initial configuration will include a high-temperature (750°C), high-pressure (7 MPa) helium loop thermally integrated with a molten fluoride salt (KF-ZrF₄) flow loop operating at low pressure (0.2 MPa) at a temperature of ~450°C. Experiment design challenges include identification of suitable materials and components that will withstand the required loop operating conditions. Corrosion and high temperature creep behavior are major considerations. The facility will include a thermal energy storage capability designed to support scaled process heat delivery for a variety of hybrid energy systems and grid stabilization strategies. Experimental results obtained from this research will also provide important data for code verification and validation (V&V) related to these systems.

INTRODUCTION

Development of the next-generation of advanced passively safe nuclear reactors is under way, demonstrating the technical and industrial vitality of nuclear energy. With a growing demand for energy and concerns about climate change [1],

nuclear energy must be included in the overall energy portfolio, as a sustainable and environmentally friendly technology [2, 3]. High temperature next-generation nuclear reactors will have reactor outlet temperatures of about 700–850°C for the first of a kind, further increased to 900–1000 °C for the nth of a kind unit. These reactors are attractive to the corporate sector because of their high-efficiency power production as well as their ability and provide high temperature process heat for various industrial applications such as hydrogen production [4] and chemical processing [5], thus expanding the range of applications of nuclear energy.

The facility described in this paper addresses technical issues associated with two advanced reactor concepts, the high-temperature gas-cooled reactor (VHTR – Very High Temperature Reactor) [6, 7] and the molten salt cooled reactor (AHTR – Advanced High Temperature Reactor) [8]. There are major technological challenges associated with these concepts that must be overcome to establish their feasibility and to develop a licensing framework. These challenges provide the motivation behind development of the thermal hydraulic loops described herein.

The VHTR is a graphite-moderated, uranium-fueled, helium-cooled thermal reactor using a direct or indirect gas cycle to convert the heat generated by nuclear fission into electrical energy. Two reactor design concepts are being studied for VHTRs: the prismatic reactor and the pebble bed reactor. The prismatic reactor has cylindrical fuel compacts stacked inside channels that are drilled into hexagonal graphite blocks. The fuel blocks are stacked firmly against each other in columns that form an annulus between an inner reflector and an outer reflector, both of which consist of rings of unfueled graphite blocks. The annular core configuration ensures inherent safety (annular core design improves conduction of decay heat to the reactor vessel for passive heat removal) under all accident and transient conditions. The pebble bed reactor

design consists of an annular vat filled with fuel spheres or pebbles that are dropped in at the top of the vat and removed at the bottom. Continuous online refueling reduces the required shut-down frequency and allows operation with very little excess reactivity. Both prismatic and pebble bed versions of the VHTR possess the same general functionality and bulk design. TRISO fuel particles are embedded in a graphite matrix to form fuel elements that occupy a tall annular or cylindrical region inside the vessel and are surrounded by graphite reflector blocks. TRISO fuel is very robust fuel form that can survive extreme high temperatures and allows operation to higher burnup compared to conventional reactor fuels [7].

The AHTR is part of the fluoride- salt-cooled high temperature reactor (FHR) class of nuclear reactors included in the advanced reactor concept program. AHTRs operate at atmospheric pressure, produce high outlet temperatures (704°C) using coated particle fuel (TRISO particles) and can potentially improve upon the attributes of other reactors [9]. An AHTR reactor core consists of coated particle fuel embedded within graphite fuel elements. Graphite reflectors provide additional moderation and core structure. Heat removed from the reactor is transferred to an intermediate salt that, in turn, is transferred to a tertiary side for power production and/or process heat applications [8]. Thus far, FHR analyses have focused mainly on power production, but, like the VHTR, the AHTR designers are looking into process heat applications, making them more attractive to industry.

Key technologies for innovative nuclear systems, such as VHTR and AHTR, present various challenges. In this study the main focus is given to addressing the testing needs for high temperature components such as high temperature heat exchangers (mainly compact heat exchangers such as printed-circuit heat exchangers) operating at prototypic intermediate heat exchanger (IHx) conditions. The initial configuration will include a high-temperature (750°C), high-pressure (7 MPa) helium loop thermally integrated with a molten fluoride salt (KF-ZrF₄) flow loop operating at low pressure (0.2 MPa) at a temperature of ~450°C. Experiment design challenges include identification of suitable materials and components that will withstand the required loop operating conditions. Experimental results obtained from this research will also provide important data for code verification and validation (V&V) which is very vital to improve the technology readiness level for the reactor concept.

HIGH TEMPERATURE COMPONENTS – MATURATION APPROACH AND PHILOSOPHY

The tools used to analyze existing reactor systems for safety and to develop the bases for the licensing of future reactor designs must be validated so that there is an assurance that the analytical results reflect the response of the system in final plant configurations. This V&V effort will require data from representative tests demonstrated in relevant environments of physical systems.

The iterative process for modeling and analysis of reactors with process heat transfer involves developing the analytical

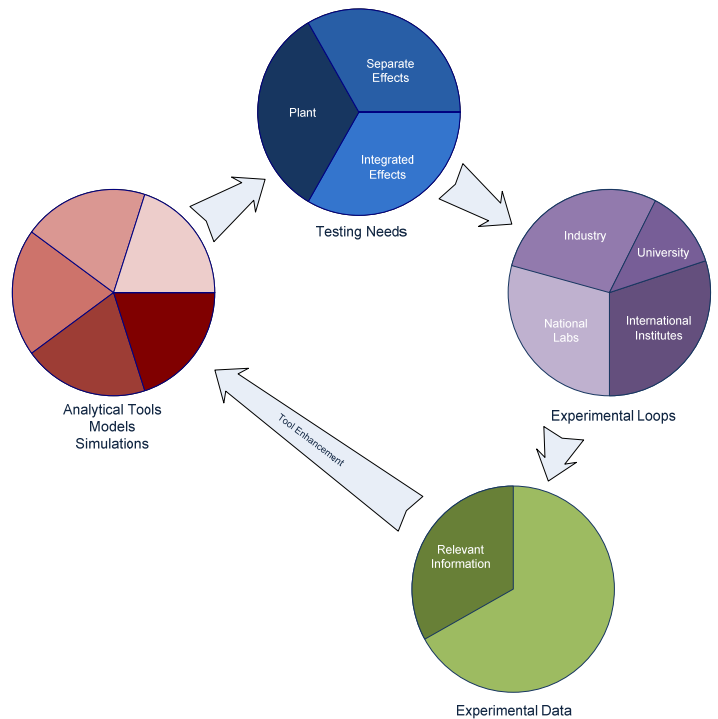


Figure 1. Interconnections between tools, testing needs and testing capabilities [10].

tools, identifying the testing needs, and developing data to support the V&V in representative tests, as shown in Figure 1.

The V&V tests will include:

- Separate effects tests—tests intended to isolate a particular phenomenon of interest from other associated phenomena that may complicate the interpretation of the results
- Integrated effects tests—tests that combine particular phenomena of interest to determine their cumulative or synergistic effects on the system
- Plant tests—tests conducted in a relevant environment such as the actual plant or a plant prototype.

These empirical test data and the derived relevant information will advance understanding of the physical systems in relevant environments, inform the licensing efforts, and help identify needed enhancements to the analytical tools. The system described in this paper will provide data from separate effects tests and some integrated effects tests.

HEAT TRANSPORT SYSTEM COUPLING

High temperature reactors are designed to increase energy efficiency in the production of electricity and provide high-temperature heat for industrial processes. At the same time, for reasons of safety and isolation of the primary reactor coolant, an intermediate heat transfer loop (IHx) is essential. Consequently, efficient transfer of energy from the reactor to the industrial application depends on the ability to incorporate effective heat exchangers between the primary reactor coolant

and the industrial process heat transport system. The need for efficiency, compactness, and safety at high temperature reactor operating conditions challenge the boundaries of existing heat exchanger technology. Compactness is especially important for current small modular reactor design concepts. Compact heat exchangers can be fabricated by a number of processes, or by a combination of processes including casting, additive manufacturing, and precisely controlled conventional welding such as laser, electron beam, or arc welding. Diffusion welding, a solid-state welding process carried out at high temperatures, is especially suitable for fabricating compact heat exchangers [11]. Diffusion bonding (the American Welding Society prefers the term diffusion welding) is defined as “A solid-state welding process wherein coalescence of the faying surfaces is produced by the application of pressure and elevated temperature. The process does not involve macroscopic deformation or relative motion of the parts; a solid filler metal may or may not be inserted” [12]. Diffusion welding is a solid-state welding process that relies on the diffusion of atoms across an interface to form a joint. At very high temperatures, diffusion rates are high, and the normal mechanisms of grain growth will cause grain boundaries to cross the interface, leaving, in the ideal case, a joint that is indistinguishable from the base metal. The integrity of the bond or the strength of the bond is very important as the heat exchanger is the main source of getting the thermal energy away from the reactor, thus the scaled heat exchanger needs to be tested in the prototypic environment. The multi-fluid loop under development will assist in meeting that objective along with providing experimental data for V&V for the heat exchangers models. Currently an experimental database for such heat exchangers with He and molten salt at the required pressures and temperatures does not exist.

FIGURES OF MERIT FOR COOLANT SELECTION

Heat transfer fluids are selected based on various properties such as melting point, vapor pressure, density, thermal conductivity, heat capacity, viscosity, and coolant chemistry. In selecting a coolant, if a certain coolant shows superior properties, the decision can be very straightforward. However, generally, each potential coolant exhibits good characteristics for some properties but poor for others. Therefore, it is very useful to develop figures of merit (FOMs) that can represent and quantify coolant thermal and chemical performance in the system of interest. The development of these FOMs is discussed in detail in reference [13]. A brief summary is provided here. Desirable characteristics for IHTL coolants include:

- **High heat transfer performance**
- **Low pumping power**
- **Low coolant volume**
- **Low quantity of structural materials**
- **Low heat loss**
- **Low temperature drop**

Corresponding to the six requirements listed above, six FOMs were developed in [13]. For example, consideration of

appropriate correlations for heat transfer coefficient and pumping power for turbulent pipe flows yields the following expression for FOM_{ht} .

$$FOM_{ht} = \frac{h}{h_o} = \left(\frac{k}{k_o}\right)^{0.6} \left(\frac{\rho}{\rho_o}\right)^{0.58} \left(\frac{C_p}{C_{p,o}}\right)^{0.4} \left(\frac{\mu}{\mu_o}\right)^{-0.47} \quad (1)$$

In this equation, the denominator of each factor represents a reference fluid property. The value of FOM_{ht} quantifies the relative heat transfer performance of a candidate coolant evaluated at the same pumping power and flow geometry. Eqn. (1) also reveals the sensitivity of this heat transfer performance criterion to the various fluid properties. The sensitivity to each property is given by the exponent of the corresponding factor. Figures of merit were also derived for the other coolant characteristics. A summary of the results is presented in Table 1. In the table, the equations for each FOM are provided in the first column and the sensitivities (exponents) associated with each fluid property are listed in the remaining columns. A comparison of FOM values for various candidate molten salt coolants is presented in Table 2. The best overall candidate based on these FOM value is LiF-NaF-KF (FLiNaK). However, KF-ZrF₄ (58-42) is a good candidate in most categories as an alternative and it has one of the lowest melting points, which reduces some of the design challenges for the test loop. Therefore KF-ZrF₄ has been selected as our baseline salt.

Table 1. Summary of figures of merit for candidate coolant fluids.

Figure of Merit	Sensitivity of Properties				
	S_k	S_ρ	S_{C_p}	S_μ	S_P
Heat transfer performance factor (FOM_{ht}): $FOM_{ht} = \frac{(k)^{0.6} \cdot (\rho)^{0.58} \cdot (C_p)^{0.4} \cdot (\mu)^{-0.47}}{R_{ht,0}}$	0.6	0.58	0.4	-0.47	0.0
Pumping factor (FOM_p): $FOM_p = \frac{\rho^{-2} \cdot C_p^{-2.8} \cdot \mu^{0.2}}{R_{p,0}}$	0.0	-2	-2.8	0.2	0.0
Coolant volume factor (FOM_{cv}): $FOM_{cv} = \frac{(\rho)^{-0.84} \cdot (C_p)^{-1.16} \cdot (\mu)^{0.1}}{R_{cv,0}}$	0.0	-0.84	-1.16	0.1	0.0
Material Volume factor (FOM_{ccv}): $FOM_{ccv} = \frac{(P) \cdot (\rho)^{-0.84} \cdot (C_p)^{-1.16} \cdot (\mu)^{0.1}}{R_{ccv,0}}$	0.0	-0.84	-1.16	0.1	1.0
Heat loss factor (FOM_{hl}): $FOM_{hl} = \frac{(k)^{0.6} \cdot (\rho)^{0.34} \cdot (C_p)^{0.06} \cdot (\mu)^{-0.44}}{R_{hl,0}}$	0.6	0.34	0.06	-0.44	0.0
Temperature drop factor (FOM_{dt}): $FOM_{dt} = \frac{(k)^{0.6} \cdot (\rho)^{0.34} \cdot (C_p)^{0.06} \cdot (\mu)^{-0.44}}{R_{dt,0}}$	0.6	0.34	0.06	-0.44	0.0

Table 2. Comparisons of FOM values for the various molten salt coolants.

Coolant	Melting Point (°C)	K (W/m K)	P (kg/m ³)	C _p (J/kg K)	μ (Pa s)	P (atm)	FOM _{th}	FOM _p	FOM _{cv}	FOM _{ccv}	FOM _{hl}	FOM _{dt}
Water (25°C)	0	0.61	997.05	4181	0.00089	1	1.00	1.00	1.00	1.00	1.00	1.00
LiF-NaF-KF	454	0.92	2020	1886	0.0029	1	0.80	2.87	1.57	1.57	0.92	0.92
NaF-ZrF ₄	500	0.49	3140	1173	0.0051	1	0.45	5.02	1.98	1.98	0.56	0.56
KF-ZrF ₄	390	0.45	2800	1046	0.0051	1	0.38	8.69	2.49	2.49	0.51	0.51
LiF-NaF-ZrF ₄	436	0.53	2920	1233	0.0069	1	0.40	5.36	2.05	2.05	0.50	0.50
LiCl-KCl	355	0.42	1520	1198	0.00115	1	0.55	14.99	3.07	3.07	0.76	0.76
LiCl-RbCl	313	0.36	1880	890	0.0013	1	0.47	23.03	3.66	3.66	0.70	0.70
NaCl-MgCl ₂	445	0.5	1680	1096	0.00136	1	0.58	16.26	3.18	3.18	0.81	0.81
KCl-MgCl ₂	426	0.4	1660	1160	0.0014	1	0.50	14.30	3.02	3.02	0.70	0.70
NaF-NaBF ₄	385	0.4	1750	1507	0.0009	1	0.71	5.66	2.04	2.04	0.88	0.88
KF-KBF ₄	460	0.38	1700	1305	0.0009	1	0.64	8.98	2.47	2.47	0.84	0.84
RbF-RbF ₄	442	0.28	2210	909	0.0009	1	0.54	14.61	3.01	3.01	0.75	0.75

One objective of the project will be to expand the data base for the thermophysical properties of this particular salt.

PRELIMINARY DESIGN OF THE MULTIPURPOSE LOOP

A process flow diagram for the multi-fluid, multi-loop test facility is shown in Fig. 2. The facility includes three thermally interacting flow loops: helium, molten salt, and steam/water. The helium loop will be initially charged from pressurized gas storage cylinders to the loop operating pressure of 7 MPa. The loop can be evacuating prior to charging for removal of air. This process can be repeated with intermediate gas venting via the deaeration vent to achieve the desired loop He purity level. Helium flow through the loop will be driven by a water-cooled centrifugal gas circulator rated for high-pressure service, with a design flow rate up to 525 LPM at 7 MPa (11,300 SLPM) and a pressure drop of 100 kPa. The circulator flow rate will be controlled by means of a variable-frequency drive coupled to the motor. The helium circulator will be designed to operate with a maximum helium temperature of 100°C. It is therefore located in the low-temperature section of the helium flow loop. The gas is preheated to intermediate temperature by flowing through a helium-to-helium recuperator which transfers heat from the higher temperature helium return flow. The high temperature portion of the flow loop is designed to handle helium temperatures up to 800°C. This temperature will be achieved using a high temperature electrical in-line gas heater (60 kW). The helium loop will include a high temperature test section for heat transfer and materials studies. Downstream of the test section, the helium gas flows through a heat exchanger where heat will be transferred to the adjacent molten salt loop using a scaled version of an intermediate heat exchanger. This heat exchanger will be a high efficiency compact microchannel PCHE. Downstream of the IHX, the helium flows through an intermediate temperature test section and the recuperator to transfer heat back to the inlet stream.

The baseline design for the He-He recuperator will also be a PCHE. In addition to its heat recuperation role, this heat exchanger can simulate an IHX for the case in which He is used as an intermediate heat transfer fluid. For tests aimed at characterizing the performance of this heat exchanger operating in He-He IHX mode, the He-salt IHX will be bypassed and the low-temperature gas heater will be used to increase the temperature on the low-temperature side of the recuperator to 400°C for prototypical IHX operation.

Downstream of the recuperator, the helium flows through a water-cooled chiller to cool it back down to the gas circulator operating temperature.

The center part of Fig. 2 shows the molten salt portion of the multi-loop facility. The loop will be charged with salt from the salt storage tank. This tank will include a heater that is designed to heat the frozen salt to a temperature above its melting point. The head space in the molten salt storage tank will be filled with inert cover gas. The vertical cantilever salt pump will be designed to operate at 420°C at low pressure (~0.2 MPa). It will provide molten salt flow rates up to 20 LPM. A standard stainless steel such as 316 should be suitable for the pump material. The entire molten salt flow loop will be heat-traced to prevent salt from freezing and causing a flow blockage. Downstream of the pump, the salt flow rate will be measured using an ultrasonic flow transducer. The salt temperature will be boosted as needed to the desired intermediate temperature using an in-line electrical auxiliary heater. A salt chemistry control section will be installed at the intermediate temperature location. The molten salt temperature will increase to ~480°C as it flows through the IHX and heat is transferred from the helium loop to the salt loop. For some studies, the IHX will not be required; an IHX bypass will enable salt flow to the high temperature test section without the pressure drop associated with the IHX. Downstream of the high temperature test section, the molten salt flows through a secondary heat exchanger (SHX), transferring heat to the

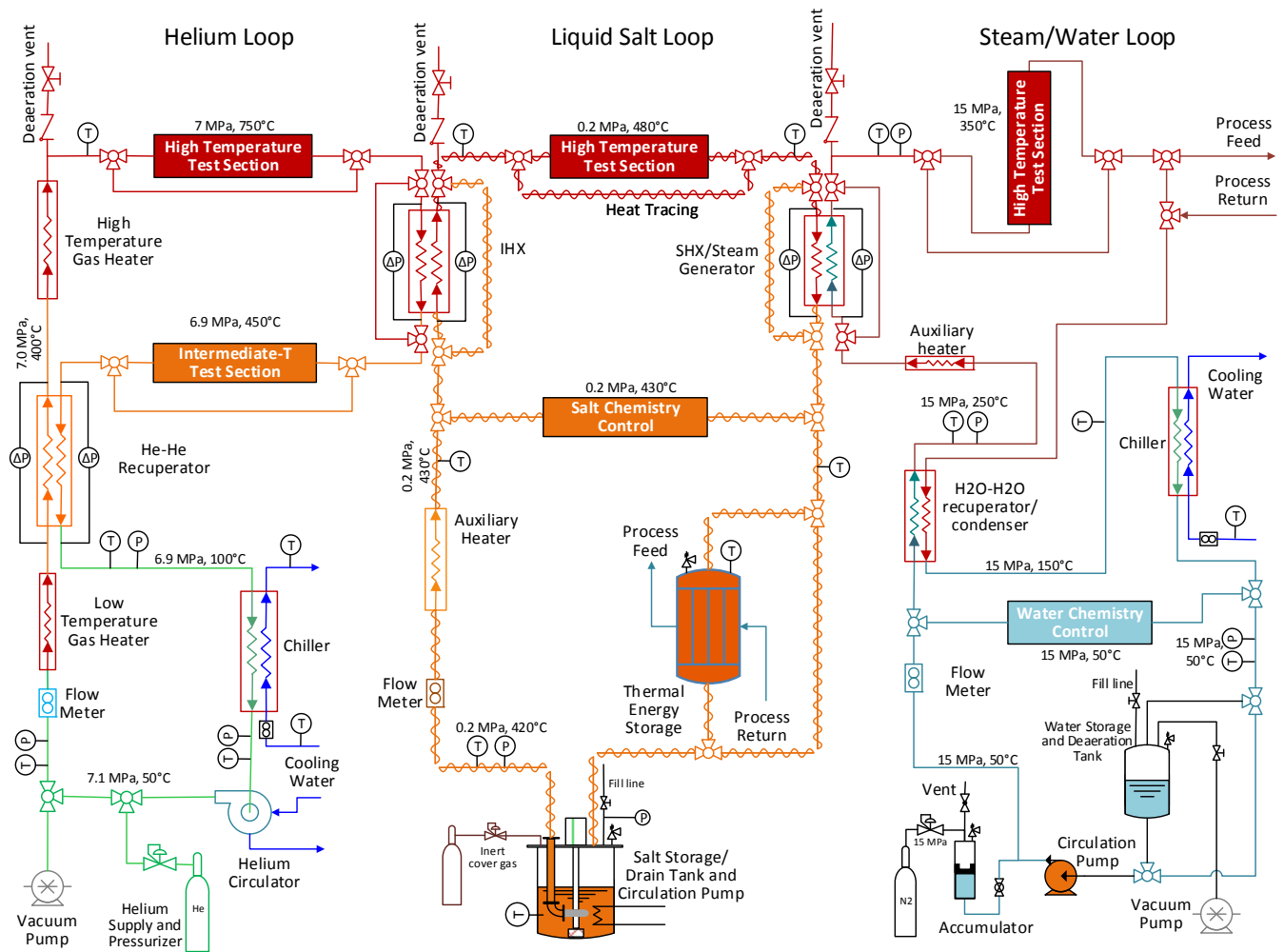


Figure 2. Process flow diagram for multi-fluid, multi-loop test facility.

tertiary steam/water loop. An SHX bypass line is also provided for cases in which the molten salt loop will be operated independently of the steam/water loop. The salt can then flow directly back to the pump or it can flow through a thermal energy storage (TES) system for process integration studies.

The right-hand side of Fig. 2 shows the steam/water tertiary loop. The SHX can serve as a steam generator or simply a single-phase heat exchanger, depending on the conditions to be simulated in the tertiary loop. For some tests, the conditions in the tertiary loop will be intended to simulate pressurized water reactor (PWR) conditions. PWR conditions will be needed for materials/corrosion studies of accident-tolerant fuels, new cladding materials, CRUD formation, etc. Alternately, at lower operating pressure, the tertiary loop can simulate the secondary side of a PWR system, with steam generation for process integration studies. The tertiary loop includes a condenser/chiller to cool the process stream back down to the pump operating temperature.

Selection of the overall scale of this facility in terms of flow rates, pump requirements, heater power, heat exchanger duty, piping size, etc. is based on a compromise between

capability and cost. With these factors in mind, the facility has been designed to support a molten salt flow rate of 1 kg/s with a temperature rise across the IHX of 50°C. Once this selection is made, the IHX heat duty is fixed. Flow rates of the remaining fluids in the multi-fluid loop can subsequently be calculated based on appropriate values of temperature change across the IHX and/or the SHX. Operating conditions, heat exchanger duties and flow rates for KF-ZrF_4 , He, H_2O liquid, supercritical CO_2 , and Na are listed in Table 3, corresponding to a KF-ZrF_4 flow rate of 1 kg/s and a ΔT across the IHX of 50°C, which yields a heat exchanger duty of 52.6 kW. Each fluid is listed with an appropriate application-oriented heat exchanger ΔT . For example, the expected temperature difference for primary helium across the IHX is $\sim 320^\circ\text{C}$ in the VHTR application. Supercritical CO_2 and sodium are included in the table due to their importance for nuclear applications. These fluids will not be employed in the initial configuration of the multi-fluid loop, however. Mass and actual volume flow rates are listed for all the fluids. Volumetric flow rates for gases are also listed in terms of standard liters per minute (SLPM).

Table 3. Flow rates based on KF-Zr4 flow of 1 kg/s, with 50°C HX delta-T.

Fluid	P	T _{mean}	HX ΔT	HX Duty	Mass flow rate	Volume flow rate	Volume flow rate	Volume flow rate
	MPa	°C	°C	kW	kg/s	L/min (actual)	SLPM	gpm
KF-ZrF ₄	0.2	~450	50	52.6	1	19.6	n/a	5.18
He	7	600	320	52.6	.0316	491	10620	n/a
H ₂ O liq	10	300	50	52.6	.185	15.5	n/a	4.10
SCO ₂	20.5	372	150	52.6	.25	89.0	7648	n/a
Na	0.2	600	50	52.6	0.83	64.4	n/a	17.0

Volume flow rates for liquids are also listed in terms of gallons per minute (gpm).

CONSTRUCTION MATERIALS

Candidate materials of construction include materials that exhibit (in varying degrees) high temperature tensile and creep strength and resistance to environmental degradation in molten salts. The current discussion is limited to metallic materials. Longer-term R&D programs will evaluate ceramic and composite designs. Issues that must be addressed during the design process include materials compatibility with both Fluoride and Chloride salts. Some of the materials options that could potentially be used for the construction of the facility are listed in Table 4. Structural materials under consideration include high temperature Ni alloys which exhibit good strength and corrosion resistance at high temperatures. Out of all the alloys listed, Alloy 800H is the only one that has been approved/codified up to 760°C per ASME code case requirements. Hastelloy N (HN) is the only material for which extensive corrosion test data that are available with fluoride

salts, mainly due to experience with the molten salt breeder reactor program at ORNL which proved the feasibility of the molten salt as a coolant in the reactor system and showed negligible corrosion at high temperature under long term-exposure. The alloys that exhibit the greatest corrosion resistance to molten salts are not codified for use in nuclear applications. Those that are currently codified are inferior, and their use would result in shorter heat exchanger life.

CORROSION AND MATERIALS DEGRADATION

The great variety of salt systems, environmental conditions, and possible materials leads to a huge test matrix in designing reactor and heat transfer systems. Experimental corrosion work is necessary as these variables are gradually reduced to final choices for system use. Experimental data provide the fundamental basis of construction codes, and it is inconceivable that a reactor system would be built without an extensive database. Such experimental work can be very expensive; however, any technique that can shorten this process and make the experimental choices more efficient is worth

Table 4. Composition of high temperature materials.

Components	Quantity in Alloy, w/o						
	617	600	800H	230	Alloy N	Alloy 242	SS 316
Nickel	44.5 min	72.0 min	30.0-35.0	57 as balance	71	65	10.0-14.0
Chromium	20.0-24.0	14.0-17.0	19.0-23.0	22	7	7.0-9.0	16.0-18.0
Iron	3.0 max	6.0-10.0	39.5 min	3 max	5 max	2.0 max	as balance
Molybdenum	8.0 - 10.0			2	16	24.0-26.0	2.0-3.0
Managanese	1.0 max	1.0 max		0.5	0.80 max	0.8 max	2.0 max
Carbon	0.05-0.15	0.15 max	0.05-0.10	0.1	0.08 max	0.03 max	0.08 max
Silicon	1.0 max	0.5 max		0.4	1 max	0.8 max	0.75 max
Sulfur	0.015 max						0.03 max
Copper	0.5 max	0.5 max			0.35 max	0.2 max	
Cobalt	10.0-15.0			5 max	0.20 max	2.5 max	
Aluminum	0.8-1.5		0.15-0.60	0.3	Al + Ti = 0.35 max	0.5 max	
Titanium	0.6 max		0.15-0.60			0.006 max	
Boron	0.006 max			0.015 max			
Tungsten				14	0.50 max		
Others	La =0.02						P = 0.045 max N = 0.10 max

Table 5. Comparison of Corrosion Rates for Alloys N and 242.

Condition	Thickness loss, μm	
	Alloy N	Alloy 242
70% HF, 910°C, 136 hrs	401	320
Cl/FI salt mixture, 700-900°C, 40 hr	36	48
5% HF, 79.4°C	508	356
10% HCl, boiling	5180 $\mu\text{m}/\text{yr}$	559 $\mu\text{m}/\text{yr}$

investigating. Recently, the development of computer codes based on fundamental thermodynamics and extensive materials databases has revolutionized the process. Experimental work is still needed, but these new tools offer a number of advantages.

One such investigation into materials of interest in molten salt systems was conducted at INL [15]. The code used for these models was ThermoCalc and its associated nickel database. The materials compared were Haynes Alloys N and 242 (see compositions in Table 4) in KF-ZrF₄ molten salt at 740°C. Although no data existed in the literature for this particular combination of materials, a report by Rothman [16] provides the data shown in Table 5 for a chloride/fluoride salt mixture. The model prediction from [15] was close to the observed corrosion rates in the chloride/fluoride salt mixture.

MATERIALS DEGRADATION

A large amount of corrosion data have been generated by ORNL and others on molten fuel salt corrosion for application in MSRs such as the Aircraft Reactor Experiment (ARE), MSRE, and the Molten Salt Breeder Reactor (MSBR) with review articles that summarize the results [17 - 23].

CORROSION MECHANISMS

The molten salt literature has identified several corrosion mechanisms, including:

- Intrinsic corrosion, with molten salt as the reactant. The mechanism is driven by the difference in free energy of formation between the salt constituents and the most susceptible transition metal corrosion product (the more negative the free energy of reaction, the more likely is the reaction).
- Corrosion by oxidizing contaminants in the molten salts, such as HF, HCl, H₂O, residual oxides of metals, or easily reducible ions, especially some polyvalent metal ions.
- Differential solubility because of thermal gradients in the molten salt system, with formation of a metal ion concentration cell that can drive corrosion.
- Galvanic corrosion, wherein metals or materials with differing electromotive potentials are maintained in electrical contact by the molten salt, driving the oxidation of the anodic material.

Molten salt technology has been used for many decades in industrial heat transfer, thermal storage, heat treatment, high-temperature electrochemical plating, and other materials processing applications. The potential utility of molten salts as

heat transfer agents was also demonstrated for nuclear reactors, as the liquid fuel in the ARE and the MSRE programs.

The issues of radiation embrittlement and intergranular cracking will not be a major concern for the secondary loop, except where the primary-to-secondary heat transfer takes place. Diffusion of tritium from the primary loop to the secondary loop will be an issue. A feature of molten fluoride salts is that they can easily dissolve passive oxide layers such as the chromium oxide film (Cr₂O₃), providing corrosion resistance for stainless steels and nickel-based alloys in many aqueous and high temperature environments. This, in fact, is the very reason fluorides are used in fluxes for many welding processes. Moisture and oxide impurities in fluorides can cause corrosion (oxidation) of the metal alloy in the molten salt.

Corrosion by the Molten Salt

Some chloride corrosion products have greater solubility in the molten chloride salt, favoring the reaction. The relative stability of fluoride compounds correlates approximately with the free energy of formation per mole fluoride, with thermodynamic stability increasing with decreasing (more negative) free energy.

Corrosion by Contaminants

While alkali and alkaline earth fluorides, and to a lesser degree the corresponding chlorides, are very stable and therefore very weak oxidants of metals, contaminants in these salts often are the cause of structural alloy corrosion [24, 25]. Dissolved contaminants in the molten salts generally increase the oxidation potential of the salt, and therefore increase the probability and rate of corrosion. Possible contaminants include water, HF or HCl, metal oxides, and dissolved polyvalent foreign cations (metal ions) that can oxidize constituents of the structural alloys.

Differential Solubility

The corrosion of soluble fluorides and chlorides may be limited by the saturation solubility of the transition metal ions in a static, isothermal salt. On the other hand, in a system with significant temperature gradients, differential solubility of corrosion products in the salt can drive persistent long-term corrosion.

Galvanic Corrosion

Molten salts are ionic fluids that can sustain electrical currents and electrochemical processes that depend on electron transfer. Molten salts can sustain the electrochemical corrosion mechanisms usually associated with aqueous systems, including galvanic corrosion. The design considerations for a molten salt coolant system may dictate the use of several different materials, which may have differing electromotive potentials (galvanic potentials) and be susceptible to galvanic corrosion.

SALT-SPECIFIC CORROSION ISSUES

Several of the fluoride and chloride salts listed in Table 2 have been studied for nuclear applications. A summary of

corrosion characteristics of some of these salts is provided below.

Corrosion in FLiNaK and FLiBe

Based on thermodynamic principles, neither FLiBe nor FLiNaK can corrode the transition metal components of structural alloys to any significant degree. However, arguments have been made that FLiNaK is inherently more corrosive to structural metals than FLiBe, based on Lewis acid-base arguments [23, 26]. As with FLiBe, the corrosion database for FLiNaK coolant salts is insufficient and needs further development for reliable selection of compatible alloys.

Corrosion in KCl-MgCl₂

Molten chloride salts have long been applied by industry for heat transfer, heat treatments, high-temperature electrochemical coatings, and other processes. The corrosion characteristics have been studied for some common structural alloys in a variety of salts.

Corrosion in KF-ZrF₄

To understand the interaction of Hastelloy N with KF-ZrF₄, specimens prepared at INL were shipped to the University of Wisconsin, for exposure to KF-ZrF₄ at high temperatures. Although a circulating loop was available at Wisconsin, these initial tests in molten KZrF salts were performed in still, molten salt. Weld specimens were made with two pieces of 0.041 in. Alloy N sheet material sandwiched between two bars of Alloy N material. For more information refer to reference [27].

SIMULINK MODEL

To aid in the design of this multipurpose facility, a dynamic system analysis code is being developed using the Matlab Simulink framework. Matlab Simulink is a graphical programming tool for modeling, simulating and analyzing dynamic system. Using this code, component models such as pipes, heat exchangers, etc. are modularized and are connected to each other to compose the flow loop through a graphical user interface (GUI). The current version of the code has a capability to analyze the steady-state thermal-hydraulic behavior of the system. This code consists of the thermal-hydraulic system component models which include the pump, pipe, heater, cooler and heat exchanger. Steady-state calculations for the designed multi-loop system are performed to evaluate the thermal-hydraulic performance and requirements of the system. In the future, the thermal storage tank model will be added to simulate interactions with hybrid energy systems.

Fig. 3 shows the Simulink GUI model for the loop simulation. The Simulink model is constructed by simply dragging, dropping and connecting the component modules. The data transferred from component to component include mass flow rate, pressure, temperature and fluid material. In this code, the quasi-static approach is employed to obtain the outlet temperature and pressure of the component. Instead of solving the partial differential conservation equations, the analytical solution of each component is implemented to calculate the outlet temperature and pressure which are transferred to the

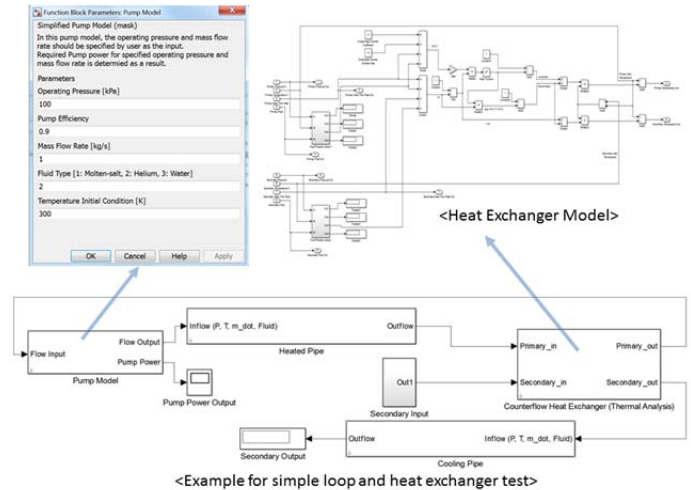


Figure 3. Matlab Simulink models of the dynamic system response analysis code.

next component. The Matlab Function Block in Matlab Simulink is used to implement the heat loss and pressure drop in the insulated pipe. Analytical solutions of the printed circuit heat exchanger are employed to model the heat exchanger as follows:

Parallel-flow PCHE:

$$\text{Primary: } T_{1,out} = T_{1,in} + (T_{2,in} - T_{1,in}) \frac{1 - e^{-NTU_1(1+R_1)}}{1+R_1}$$

$$\text{Secondary: } T_{2,out} = T_{1,in} + (T_{2,in} - T_{1,in}) \frac{1+R_1 e^{-NTU_1(1+R_1)}}{1+R_1}$$

Counter-flow PCHE:

$$\text{Primary: } T_{1,out} = T_{1,in} + (T_{2,in} - T_{1,in}) \frac{1 - e^{-NTU_1(1-R_1)}}{1-R_1 e^{-NTU_1(1-R_1)}}$$

$$\text{Secondary: } T_{2,out} = T_{1,in} + (T_{2,in} - T_{1,in}) \frac{1-R_1}{1-R_1 e^{-NTU_1(1-R_1)}}$$

For a specified inlet pressure and temperature of each component, the thermo-physical properties of the fluid are determined based on the REFPROP database [14].

CONCLUSIONS

A preliminary conceptual design of a high-temperature multi-fluid, multi-loop test facility for nuclear applications has been presented. The loop will utilize advanced high-temperature compact printed-circuit heat exchangers (PCHEs) operating at prototypic intermediate heat exchanger (IHX) conditions. The initial configuration will include a high-temperature (750°C), high-pressure (7 MPa) helium loop thermally integrated with a molten fluoride salt (KF-ZrF₄) flow loop operating at low pressure (0.2 MPa) at a temperature of ~450°C. Experimental results obtained from this research will provide important data for code verification and validation (V&V) related to these systems.

Design challenges such as identification of suitable materials and components that will withstand the required loop operating conditions have been presented. Corrosion and high

temperature creep behavior are also major considerations. Figures of merit for selection of appropriate heat transfer fluids have been developed and evaluated for several candidate fluids. A review of corrosion mechanisms and salt-specific corrosion issues has been presented.

REFERENCES

1. Kharecha, P. A., and Hansen, J. E., "Prevented Mortality and Greenhouse Gas Emissions from Historical and Projected Nuclear Power," *Environmental Science and Technology*, Vol. 47, No. 9, pp. 4889-4895, 2013.
2. Friedrich, R., Rabl, A., and Spadaro, J. V., "Quantifying the Costs of Air Pollution: The ExternE Project of the EC," *Pollution Atmospherique*, pp. 77-104, Dec. 2001.
3. Rabl, A. and Rabl, V. A., "External Costs of Nuclear: Greater or Less than the Alternatives?" *Energy Policy*, Vol. 57, pp. 575-584, 2013.
4. O'Brien, J. E., McKellar, M. G., Harvego, E. A., and Stoots, C. M., "High-Temperature Electrolysis for Large-Scale Hydrogen and Syngas Production from Nuclear Energy – Summary of System Simulation and Economic Analyses," *International Journal of Hydrogen Energy*, Vol. 35, Issue 10, pp. 4808-4819, May 2010.
5. HTGR Industrial Application Functional and Operational Requirements, INL External Report, INL/EXT-10-19706, August, 2010.
6. The Very High Temperature Reactor: A Technical Summary, MPR Associates, Sponsor: US Department of Energy, 47 p., June 2004.
7. NGNP Research and Development Status, INL External Report, INL/EXT-10-19259, August 2010.
8. Forsberg, C. W., Peterson, P., and Pickard, P. S., "Molten-Salt-Cooled Advanced High Temperature Reactor for Production of Hydrogen and Electricity," *Nuclear Technology*, Engineering International, Vol. 144, No. 3, pp.289-302, 2003.
9. Scarlat, R. O., and Peterson, P. F., "The Current Status of Fluoride Salt Cooled High Temperature Reactor (FHR) Technology and its Overlap with HIF Target Chamber Concepts," *Nuc Inst. And Methods in Physics Res. A*, Vol. 733, pp. 57-64, 2014.
10. Sabharwall, P., Collins, J., Clark, D., Siahpush, A., Phoenix, W., McKellar, M., and Patterson, M., "Technology Development Roadmap for the Advanced High Temperature Reactor Secondary Heat Exchanger," INL External Report INL/EXT-12-26219, Sept., 2012.
11. Clark, D. E., Mizia, R. E., Glazoff, M. V., and Patterson, M. W., "Diffusion Welding of Compact Heat Exchangers for Nuclear Applications," INL Technical Report, INL/CON-11-23250, June, 2012.
12. Sabharwall, P., Clark, D. E., Mizia, R. E., Glazoff, M. V., and McKellar, M. G., "Diffusion-Welded Microchannel Heat Exchanger for Industrial Processes," *J. Thermal Sci. Appl.*, Vol. 5, No. 1, 12 p., 2012.
13. Sabharwall, P., Kim, E.S., McKellar, M., Anderson, N.A., and Patterson, M., "Process Heat Exchanger options for Fluoride Salt High Temperature Reactor," INL External Report, INL/EXT-11-21584, Idaho National Laboratory, Idaho, June, 2011.
14. National Institute of Standards and Technology (NIST), (2013), Reference Fluid Thermodynamic and Transport Properties (REFPROP), U.S. Department of Commerce, <http://www.nist.gov/srd/nist23.cfm>.
15. Glazoff, M. V., 2012, Thermodynamic Assessment of Hot Corrosion Mechanisms of Superalloys Hastelloy N and Haynes 242 in Eutectic Mixture of Molten Salts KF and ZrF₄, INL/EXT-12-24617, Idaho National Laboratory, February 2012.
16. Rothman, M. R., Haynes International, and R. Baden, Robert Zapp Werkstofftechnik GmbH, 1991, "Haynes 242 Alloy for Process Industry Applications at Elevated Temperature," *ACHEMA. Frankfurt, Germany, June 1991*.
17. Grimes, W. R., E. G. Bohlmann, A. S. Meyer, and J. M. Dale, 1972, "Fuel Can Coolant Chemistry," Chapter 5 in M. W. Rosenthal, P. N. Haubenreich, and R. B. Briggs, *The Development Status of Molten-Salt Breeder Reactors*, ORNL-4812, Oak Ridge National Laboratory.
18. McCoy, H. E., Jr., 1967, *An Evaluation of the Molten Salt Reactor Experiment Hastelloy N Surveillance Specimens-First Group*, ORNL-TM-1997, Oak Ridge National Laboratory, Oak Ridge, TN, November 1967.
19. McCoy, H. E., Jr., 1969, *An Evaluation of the Molten Salt Reactor Experiment Hastelloy N Surveillance Specimens-Second Group*, ORNL-TM-2359, Oak Ridge National Laboratory, Oak Ridge, TN, February 1969.
20. McCoy, H. E., Jr., 1970, *An Evaluation of the Molten Salt Reactor Experiment Hastelloy N Surveillance Specimens-Third Group*, ORNL-TM-2647, Oak Ridge National Laboratory, Oak Ridge, TN, January 1970.
21. McCoy, H. E., Jr., 1971, *An Evaluation Of The Molten-Salt Reactor Experiment Hastelloy N Surveillance Specimens - Fourth Group*, ORNL/TM-3063, March 1971.
22. McCoy, H. E., Jr., 1978, *Status of Materials Development for Molten-Salt Reactors*, ORNL/TM-5920, January 1978.
23. Williams, D. F., L. M. Toth, and K. T. Clarno, 2006, *Assessment of Candidate Molten Salt Coolants for the Advanced High-Temperature Reactor (AHTR)*, ORNL/TM-2006/12, Oak Ridge National Laboratory.
24. Ozeryanaya, I. N., 1985, "Corrosion of Metals by Molten Salts in Heat-Treatment Processes," *Metal Science and Heat Treatment*, Vol. 27, No. 3, pp. 184-188.
25. White, S. H., 1983, "Halides," *Molten Salt Techniques*, Vol. 1, Chapter 2, D. G. Lovering and R. J. Gale, editors, Plenum Press, New York.
26. Ingersoll, D. T., C. W. Forsberg, and P. E. MacDonald, 2006, *Trade Studies on the Liquid-Salt-Cooled Very High-Temperature Reactor: Fiscal Year 2006 Progress Report*, ORNL/TM-2006/140, Oak Ridge National Laboratory, Oak Ridge, TN, February 2006.
27. Clark, D. E., R. E. Mizia, P. Sabharwall, M. G., McKellar, 2012, "Diffusion Welding of Alloys for Molten Salt

Service – Status Report,” Idaho National Laboratory,
INL/EXT-12-24589, September 2012.